Journal of
Materials Chemistry C

Materials for optical, magnetic and electronic devices

Accepted Manuscript

This article can be cited before page numbers have been issued, to do this please use: M. Zhang, L. Chen, X. Xu, L. Zhao, S. Wang, J. Ding and L. Wang, *J. Mater. Chem. C*, 2019, DOI: 10.1039/C9TC03013A.

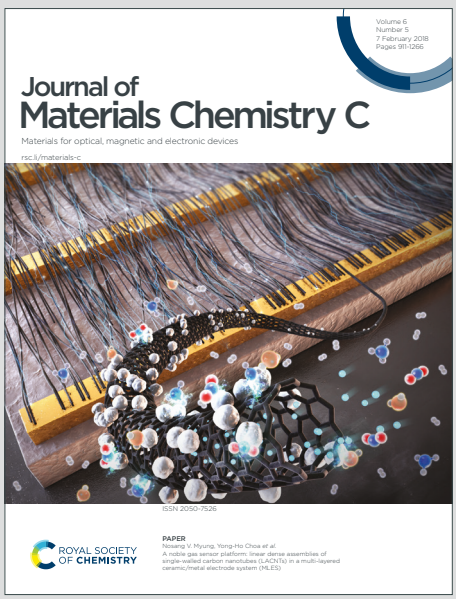

ROYAL SOCIETY OF CHEMISTRY

rsc.li/materials-c

View Article Online
DOI: 10.1039/C9TC03013A

Solution Processible Triphenylphosphine-Oxide-Cored Dendritic Hosts Featuring Thermally Activated Delayed Fluorescence for Power-Efficient Blue Electrophosphorescent Devices

Mingming Zhang,[a,b] Liang Chen,[a,b] Xiushang Xu,[a] Lei Zhao,[a] Shumeng Wang,[a] Junqiao Ding,*[,a,b] Lixiang Wang*[,a,b]

[a] *State Key Laboratory of Polymer Physics and Chemistry, Changchun Institute of Applied Chemistry, Chinese Academy of Sciences, Changchun 130022, P. R. China*

[b] *University of Science and Technology of China, Hefei 230026, P. R. China*

Keywords: PhOLEDs; dendrimer; TADF; blue; triphenylphosphine oxide

View Article Online
DOI: 10.1039/C9TC03013A

Abstract

Based on oligocarbazole, carbazole/acridine hybrid and oligoacridine as the dendron, a series of solution processible triphenylphosphine-oxide-cored dendrimers denoted as 3CzCz-PO, 3AcCz-PO, and 3AcAc-PO have been designed and synthesized, respectively. With the increasing electron-donating ability from the periphery dendron, the singlet-triplet splitting (ΔE_{ST}) is found to be gradually reduced from 0.35 eV of 3CzCz-PO to 0.22 eV of 3AcCz-PO and 0.20 eV of 3AcAc-PO while remaining high triplet energy (T_1) around 2.9 eV. As a result, 3AcAc-PO exhibits an obvious thermally activated delayed fluorescence (TADF) with a lifetime of 1.0 μs. When used as the host for the blue phosphor $Ir(mpim)_3$, the corresponding solution-processed devices reveal a peak power efficiency of 46.4 lm/W. An about 57% improvement is obtained for 3AcAc-PO compared with the non-TADF host H2 (29.6 lm/W). The results clearly manifest the superiority of solution processible dendritic TADF hosts in power-efficient blue electrophosphorescent devices.

View Article Online
DOI: 10.1039/C9TC03013A

1. Introduction

Solution-processed phosphorescent organic light-emitting diodes (s-PhOLEDs) have attracted considerable attention because of their possibility to realize a near unity internal quantum efficiency and compatibility with cost-effective wet methods (e.g. inkjet printing and spin-coating).[1-5] Given the strong concentration quenching caused by triplet−triplet annihilation (TTA), phosphorescent dyes are usually doped into solution processible hosts, such as small molecules,[6-10] dendrimers[8, 11-14] and polymers[8, 15, 16]. Among them, dendrimers can achieve a trade-off between high triplet energy (T_1) and shallow highest occupied molecular orbital (HOMO) energy level.[17] Thus they are believed to be one of the most promising solution processible hosts especially for power-efficient blue s-PhOLEDs. For example, with oligocarbazole as the dendron and *N*-phenylcarbazole as the core, a dendrimer H2 (Figure 1) was reported to host the typical blue phosphor FIrpic. The corresponding devices gave a peak power efficiency (PE) of 15.4 lm/W, which was about 86% higher than that of PVK.[17] Moreover, when another high-energy-level blue phosphor FIr-*p*-OC8 was developed to match the dendritic H2 host to avoid the unwanted hole scattering, the PE was almost doubled to 34.2 lm/W.[18] And this further led to the successful fabrication of solution-processed white devices with comparative efficiency to the fluorescent tubes.

On the other hand, thermally activated delayed fluorescence (TADF) featured small molecules have been widely used as the hosts to sensitize blue phosphors in vacuum-deposited electrophosphorescent devices.[19-28] Because of extremely small singlet-triplet gap ($\Delta E_{ST} < 0.3$ eV), their energy level of the lowest singlet excited state (S_1) could be

View Article Online
DOI: 10.1039/C9TC03013A

easily tuned to locate close to that of T_1 of a phosphorescent guest. Due to the favored charge injection, the decreased driving voltage and improved PE are within our expectation for such TADF hosts compared with the conventional counterparts. For instance, Liao et al. demonstrated a spiro-based TADF host Tri-o-2PO for a sky-blue phosphor Ir-817, revealing a low turn-on voltage (V_{on}) (at 1 cd/m^2) of 2.94 V and a high PE of 58.2 lm/W.[28]

With these ideas in mind, here we report the realization of power-efficient blue s-PhOLEDs by endowing the dendritic host with a TADF feature. As shown in Figure 1, three hosts named as 3CzCz-PO, 3AcCz-PO and 3AcAc-PO are developed from H2 according to several considerations: (i) Instead of *N*-phenylcarbazole, the triphenylphosphine oxide core is adopted as the acceptor for its weak electron-withdrawing ability and π-conjugation breaking to ensure high T_1;[29] (ii) Different kinds of dendrons including oligocarbazole, carbazole/acridine hybrid and oligoacridine are selected as the donor to modulate the intramolecular charge transfer (CT) character. Based on this design, the ΔE_{ST} of the resultant dendrimers is gradually reduced following a sequence of 3CzCz-PO > 3AcCz-PO > 3AcAc-PO. Consequently, 3AcAc-PO shows an obvious delayed fluorescence with a lifetime of about 1.0 μs. When used as the host for Ir(mpim)$_3$, the solution-processed blue electrophosphorescent devices obtain a maximum PE of 46.4 lm/W. The value is much higher than H2-based devices (29.6 lm/W), clearly indicating the superiority of TADF hosts in blue s-PhOLEDs.

2. Results and discussion

2.1 Synthesis and characterization

View Article Online
DOI: 10.1039/C9TC03013A

We synthesized the triphenylphosphine-oxide-cored dendrimers according to the synthetic route depicted in Scheme S1. Starting from 1,4-dibromobenzene, the corresponding mono Grignard reagent was firstly prepared, which then reacted with $POCl_3$ to afford tris(4-bromophenyl)phosphine oxide). Finally, Pd-catalyzed C–N cross-coupling was performed between such a key intermediate and previously reported oligocarbazole (CzCz)[30], carbazole/acridine hybrid (AcCz)[31] or oligoacridine (AcAc)[31] to produce the target dendrimers with an acceptable moderate yield of 46-57%. The molecular structures of 3CzCz-PO, 3AcCz-PO and 3AcAc-PO were identified by mass spectrometry, ^{1}H, ^{13}C and ^{31}P NMR spectroscopy and elemental analysis. They show good thermal stability with a decomposition temperature (T_d) above 400 °C (Figure S1). And the glass transition temperature (T_g) is detected to be 276 °C for 3CzCz-PO and 257 °C for 3AcCz-PO. Also, their solubility is good in common organic solvents (e.g. tetrahydrofuran, chloroform, chlorobenzene and toluene), ensuring the high-quality film generation via solution processing.

2.2 Photophysical properties

The UV-Vis absorption in dichloromethane, fluorescence and phosphorescence spectra in the neat films of 3CzCz-PO, 3AcCz-PO and 3AcAc-PO are shown in Figure 2. Compared with the donor and acceptor fragments (Figure S2), the absorption bands in the range of 250 – 400 nm can be reasonably attributed to the π–π* and n-π* transitions of the peripheral dendrons, while the CT absorption is too weak to be distinguished. Ongoing from 3CzCz-PO to 3AcCz-PO and 3AcAc-PO, the emission

View Article Online
DOI: 10.1039/C9TC03013A

peak is found to be red-shifted from 420 to 454 and 467 nm. Correspondingly, the full width at half maxima (FWHM) is up from 69 to 84 and 97 nm. With respect to 3CzCz-PO, the stronger CT observed in 3AcCz-PO and 3AcAc-PO may be from the increased electron-donating capability after the replacement of carbazole by acridine. This is further confirmed by the broader and structureless phosphorescence spectra of 3AcCz-PO and 3AcAc-PO relative to 3CzCz-PO. Furthermore, they all have a T_1 around 2.9 eV, higher than most of blue phosphors. Combined with S_1 estimated from the fluorescence onset, the ΔE_{st} is determined to be down from 0.35 eV of 3CzCz-PO to 0.22 eV of 3AcCz-PO and 0.20 eV of 3AcAc-PO (Table 1). The results mean the great potential of 3AcAc-PO, which is able to act as the solution processible host to realize power-efficient blue s-PhOLEDs.

To demonstrate whether they are TADF emitters, the transient photoluminescence (PL) spectra were also measured at 298 K. It is worth noting that 3CzCz-PO exhibits a strong prompt but negligible delayed fluorescence even under an O_2-free condition (Figure 3). By contrast, a distinct delayed component is observed for 3AcCz-PO and 3AcAc-PO, giving an excited state lifetime of 1.5 and 1.0 μs, respectively. The different TADF behaviors are understandable when considering the decreased ΔE_{st} to promote the T_1-to-S_1 upconversion. Additionally, the delayed fluorescence of 3AcCz-PO and 3AcAc-PO can be partly or completely quenched by O_2 (Figure S3), indicative of their TADF nature.

2.3 Electrochemical properties

View Article Online
DOI: 10.1039/C9TC03013A

The electrochemical behavior of dendrimers 3CzCz-PO, 3AcCz-PO and 3AcAc-PO were investigated with cyclic voltammetry (CV). All of them show quasi-reversible oxidation waves upon the positive scan, and no reduction signals appear in the negative scan in dichloromethane (Figure 4). With ferrocene/ferrocenium (Fc/Fc^+) as the reference, the HOMO and LUMO levels are determined to be −5.40/-2.25 eV, −5.18/-2.29 eV and −5.13/-2.21 eV for 3CzCz-PO, 3AcCz-PO and 3AcAc-PO, respectively. The values correlate well with the theoretical simulation. As presented in Figure 5, the LUMO is localized on the triphenylphosphine oxide core, whereas the HOMO mainly distributes over the outer dendrons but with a different delocalization degree. The observation can be tentatively ascribed to the different torsion angle θ_1 between the dendron and the phenyl linkage together with θ_2 between the carbazole and/or acridine moieties in the dendron (Figure S4). As a result of the enhanced θ_1/θ_2 from $52.8^o/56.3^o$ to $90.2^o/56.3^o$ and $88.4^o/90.2^o$, the HOMO delocalization exhibits a decreased trend following a sequence of 3CzCz-PO > 3AcCz-PO > 3AcAc-PO. It should be noted that all the three dendrimers possess close LUMO levels owing to the same used core. Meanwhile, with the increasing dendron's electron donating ability from oligocarbazole to carbazole/acridine hybrid and oligoacridine, an upshifted trend for their HOMO levels is observed from 3CzCz-PO to 3AcCz-PO and 3AcAc-PO. This is beneficial for the hole injection and thus low driving voltage, which will be discussed later.

2.4 Electroluminescent Properties

View Article Online
DOI: 10.1039/C9TC03013A

In order to investigate their electroluminescent (EL) properties, solution-processed nondoped devices were firstly fabricated with 3CzCz-PO, 3AcCz-PO or 3AcAc-PO as the emitting layer (EML) independently. The device configuration is ITO/PEDOT:PSS (40 nm)/EML (40 nm)/TSPO1 (5 nm)/TmPyPB (45 nm)/LiF (1 nm)/Al (100 nm), where PEDOT:PSS, TmPyPB and TSPO1 serve as the hole-injection layer, electron-transporting layer and exciton blocking layer, respectively (Figure S5).

The EL characteristics are presented in Figure 6 and summarized in Table 2. Similar to the PL counterparts, the EL spectra are becoming more and more broad, and the corresponding Commission Internationale de L'Eclairag (CIE) coordinates are red-shifted from (0.18, 0.10) of 3CzCz-PO to (0.20, 0.21) of 3AcCz-PO and (0.21, 0.27) of 3AcAc-PO (Figure 6a).. In addition, both the current density–voltage (*J*-*V*) and luminance–voltage (*L*-*V*) curves move towards a negative voltage from 3CzCz-PO to 3AcCz-PO and 3AcAc-PO (Figure 6b). As mentioned above, the elevated HOMO levels are anticipated to facilitate the hole injection, thus leading to the reduced driving voltage. Consequently, 3AcAc-PO obtains the best device performance among these three dendrimers (Figure 6c and 6d), revealing a peak EQE of 6.7% (13.7 cd/A, 12.7 lm/W).

We note that the luminescent performance of 3AcAc-PO is not as good as that of previously-reported TADF emitters[32-35] due to its poor PL quantum yield (PLQY) of 0.33. However, it may be a promising host for blue phosphors in terms of its high T_1 and low ΔE_{st}. To verify this point, blue s-PhOLEDs were subsequently assembled by further doping $Ir(mpim)_3$ into 3AcAc-PO as the EML with an optimized content of 20

View Article Online
DOI: 10.1039/C9TC03013A

wt.% (Table S2 and Figure S6). Under the same condition, a control device was also prepared based on the non-TADF host H2 instead of 3AcAc-PO. As can be clearly seen, a bright sky-blue EL only from $Ir(mpim)_3$ is observed with CIE coordinates of (0.21, 0.44). There is no additional emission from 3AcAc-PO (Figure 7a), manifesting complete energy transfer attributable to the good overlap between the absorption of $Ir(mpim)_3$ and the PL of 3AcAc-PO (Figure S7). In comparison to H2, most importantly, the luminance and current density at the same driving voltage for 3AcAc-PO are significantly enhanced (Figure 7b). Ongoing from H2 to 3AcAc-PO, the V_{on} is decreased from 3.0 V to 2.6 V. Accordingly, the maximum luminance, CE, PE and EQE are increased from 13261 cd/m^2, 30.7 cd/A, 29.6 lm/W and 11.9% to 25815 cd/m^2, 40.7 cd/A, 46.4 lm/W and 15.8%, respectively (Figure 7c and 7d). The low ΔE_{st} as well as the higher film PLQY (0.66 for 3AcAc-PO : 20 wt.% $Ir(mpim)_3$ Vs 0.53 for H2 : 20 wt.% $Ir(mpim)_3$) may be responsible to the superior device performance of 3AcAc-PO to H2, which is among the highest ever reported for solution-processed blue PhOLEDs (Table S3).

3. Conclusion

In conclusion, solution processible triphenylphosphine-oxide-cored dendritic hosts featuring TADF have been demonstrated for power-efficient blue electrophosphorescent devices. By tuning the electron-donating ability of the periphery dendron combined with the triphenylphosphine oxide core, a distinct delayed fluorescence could be observed for 3AcAc-PO. It shows not only high T_1 to confine the

View Article Online
DOI: 10.1039/C9TC03013A

triplet excitons on blue phosphor, but also low ΔE_{st} to favor charge injection and transporting. Consequently, solution processed blue electrophosphorescent devices based on 3AcAc-PO achieve lower driving voltage and higher PE relative to the non-TADF host H2. We believe our study can promote further development of dendritic hosts towards power-efficient blue s-PhOLEDs.

Nomenclatures: The abbreviations used for molecules are as follows. [Bis(4,6-difluorophenyl)-pyridinato-N,C^2]-picolinate (FIrpic), poly(9-vinylcarbazole) (PVK), tris[1-(3,5-diisopropylbiphenyl-4-yl)-2-phenyl-1*H*-imidazole] iridium(III) (Ir-817), tris(mesityl-2-phenyl-1*H*-imidazole)iridium(III) [$Ir(mpim)_3$], poly(3,4-ethylenedioxythiophene:poly(styrenesulfonate) (PEDOT:PSS), diphenyl(4-(triphenylsilyl)phenyl)phosphine oxide (TSPO1), 1,3,5-tri(m-pyrid-3-yl-phenyl)benzene (1,3,5-tri(m-pyrid-3-yl-phenyl)benzene).

Supporting Information:

Experimental section including general information, device fabrication and testing as well as synthesis; TGA and DSC plots; transient PL spectra under nitrogen and oxygen; device configuration; ^1H, ^{13}C, ^{31}P NMR and MALDI-TOF spectra. This material is available free of charge via the Internet at http://pubs.rsc.org.

Author Information:

Corresponding authors: junqiaod@ciac.ac.cn; lixiang@ciac.ac.cn

View Article Online
DOI: 10.1039/C9TC03013A

Notes:

The authors declare no competing financial interest.

Acknowledgments:

The authors are grateful for the financial support from the National Key Research and Development Program (2016YFB0401301), the 973 Project (2015CB655001), and the National Natural Science Foundation of China (Nos. 51873205 and 51573183).

References:

1. C. Liu, Q. Fu, Y. Zou, C. Yang, D. Ma and J. Qin, *Chem. Mater.*, 2014, **26**, 3074-3083.
2. C.-F. Liu, Y. Jiu, J. Wang, J. Yi, X.-W. Zhang, W.-Y. Lai and W. Huang, *Macromolecules*, 2016, **49**, 2549-2558.
3. S. Shao, J. Ding and L. Wang, *Acta Polym. Sin.*, 2018, **2**, 198-216.
4. H. Zheng, Y. Zheng, N. Liu, N. Ai, Q. Wang, S. Wu, J. Zhou, D. Hu, S. Yu, S. Han, W. Xu, C. Luo, Y. Meng, Z. Jiang, Y. Chen, D. Li, F. Huang, J. Wang, J. Peng and Y. Cao, *Nat. Commun.*, 2013, **4**, 1971.
5. M. A. Baldo, D. F. O'Brien, Y. You, A. Shoustikov, S. Sibley, M. E. Thompson and S. R. Forrest, *Nature*, 1998, **395**, 151.
6. S. Gong, Q. Fu, W. Zeng, C. Zhong, C. Yang, D. Ma and J. Qin, *Chem. Mater.*, 2012, **24**, 3120-3127.
7. K. S. Yook and J. Y. Lee, *Adv. Mater.*, 2014, **26**, 4218-4233.

View Article Online
DOI: 10.1039/C9TC03013A

8. W. Li, J. Li and M. Wang, *Isr. J. Chem.*, 2014, **54**, 867-884.

9. S. K. Jeon, H.-J. Park and J. Y. Lee, *Acs Appl. Mater. Interfaces*, 2018, **10**, 5700-5705.

10. S. Ye, Y. Liu, J. Chen, K. Lu, W. Wu, C. Du, Y. Liu, T. Wu, Z. Shuai and G. Yu, *Adv. Mater.*, 2010, **22**, 4167-4171.

11. W. Jiang, Z. Ge, P. Cai, B. Huang, Y. Dai, Y. Sun, J. Qiao, L. Wang, L. Duan and Y. Qiu, *J. Mater. Chem.*, 2012, **22**, 12016.

12. Z. A. Hasan, K. L. Woon, W. S. Wong, A. Ariffin and S.-A. Chen, *J. Lumin.*, 2017, **183**, 150-158.

13. X. Xu, X. Yang, J. Zhao, G. Zhou and W.-Y. Wong, *Asian J. Org. Chem.*, 2015, **4**, 394-429.

14. X. Wang, S. Wang, Z. Ma, J. Ding, L. Wang, X. Jing and F. Wang, *Adv. Funct. Mater.*, 2014, **24**, 3413-3421.

15. F. Dumur, *Org. Electron.*, 2015, **25**, 345-361.

16. S. Shao, J. Ding, T. Ye, Z. Xie, L. Wang, X. Jing and F. Wang, *Adv. Mater.*, 2011, **23**, 3570-3574.

17. J. Ding, B. Zhang, J. Lu, Z. Xie, L. Wang, X. Jing and F. Wang, *Adv. Mater.*, 2009, **21**, 4983-4986.

18. S. Wang, L. Zhao, B. Zhang, J. Ding, Z. Xie, L. Wang and W. Y. Wong, *iScience*, 2018, **6**, 128-137.

19. M. Y. Wong and E. Zysman-Colman, *Adv. Mater.*, 2017, **29**, 1605444.

20. Z. Yang, Z. Mao, Z. Xie, Y. Zhang, S. Liu, J. Zhao, J. Xu, Z. Chi and M. P.

View Article Online
DOI: 10.1039/C9TC03013A

Aldred, *Chem. Soc. Rev.*, 2017, **46**, 915-1016.

21. Y. Im, M. Kim, Y. J. Cho, J.-A. Seo, K. S. Yook and J. Y. Lee, *Chem. Mater.*, 2017, **29**, 1946-1963.
22. Y. Liu, C. Li, Z. Ren, S. Yan and M. R. Bryce, *Nat. Rev. Mater.*, 2018, **3**, 18020.
23. X. Liang, Z.-L. Tu and Y.-X. Zheng, *Chem. Eur. J.*, 2019, **25**, 5623-5642.
24. J. Wang, C. Jiang, C. Liu, H. Liu and C. Yao, *Mater. Lett.*, 2018, **233**, 149-152.
25. D. Zhang, M. Cai, Z. Bin, Y. Zhang, D. Zhang and L. Duan, *Chem. Sci.*, 2016, **7**, 3355-3363.
26. C.-C. Lin, M.-J. Huang, M.-J. Chiu, M.-P. Huang, C.-C. Chang, C.-Y. Liao, K.-M. Chiang, Y.-J. Shiau, T.-Y. Chou, L.-K. Chu, H.-W. Lin and C.-H. Cheng, *Chem. Mater.*, 2017, **29**, 1527-1537.
27. C. Li, X. Fan, C. Han and H. Xu, *J. Mater. Chem. C*, 2018, **6**, 6747-6754.
28. Y.-K. Wang, Q. Sun, S.-F. Wu, Y. Yuan, Q. Li, Z.-Q. Jiang, M.-K. Fung and L.-S. Liao, *Adv. Funct. Mater.*, 2016, **26**, 7929-7936.
29. S. O. Jeon and J. Y. Lee, *J. Mater. Chem.*, 2012, **22**, 4233-4243.
30. D. Xia, B. Wang, B. Chen, S. Wang, B. Zhang, J. Ding, L. Wang, X. Jing and F. Wang, *Angew. Chem., Int. Ed.*, 2014, **53**, 1048-1052.
31. X. Wang, S. Wang, J. Lv, S. Shao, L. Wang, X. Jing and F. Wang, *Chem. Sci.*, 2019, **10**, 2915-2923.
32. X. Ban, W. Jiang, T. Lu, X. Jing, Q. Tang, S. Huang, K. Sun, B. Huang, B. Lin and Y. Sun, *J. Mater. Chem. C*, 2016, **4**, 8810-8816.
33. J. Luo, S. Gong, Y. Gu, T. Chen, Y. Li, C. Zhong, G. Xie and C. Yang, *J. Mater.*

View Article Online
DOI: 10.1039/C9TC03013A

Chem. C, 2016, **4**, 2442-2446.

34. K. Matsuoka, K. Albrecht, A. Nakayama, K. Yamamoto and K. Fujita, *Acs Appl. Mater. Interfaces*, 2018, **10**, 33343-33352.

35. X. Ban, W. Jiang, K. Sun, B. Lin and Y. Sun, *Acs Appl. Mater. Interfaces*, 2017, **9**, 7339-7346.

View Article Online
DOI: 10.1039/C9TC03013A

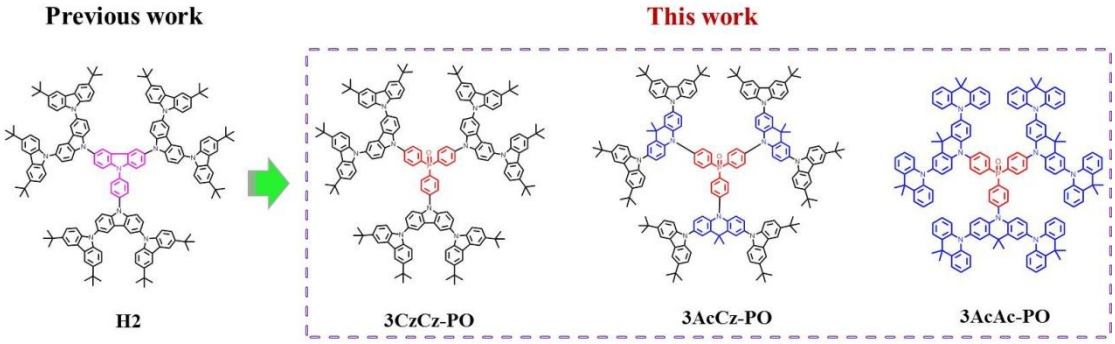

Figure 1. Molecular structures of the dendrimers 3CzCz-PO, 3AcCz-PO and 3AcAc-PO.

View Article Online
DOI: 10.1039/C9TC03013A

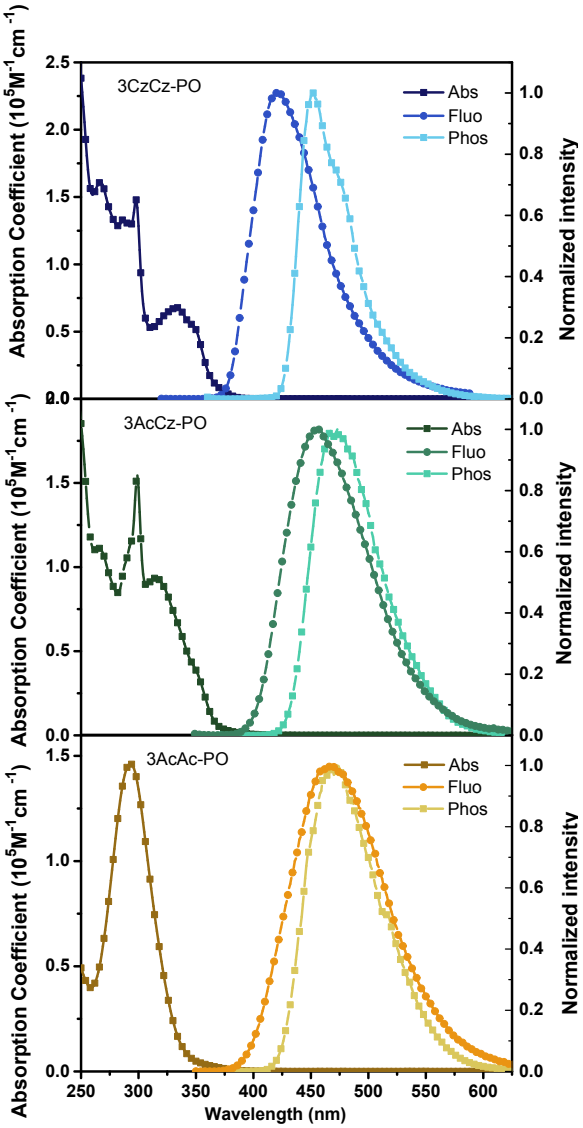

Figure 2. UV-Vis absorption in CH_2Cl_2, fluorescence (298K) and phosphorescence (77K) spectra in neat films for 3CzCz-PO, 3AcCz-PO and 3AcAc-PO.

View Article Online
DOI: 10.1039/C9TC03013A

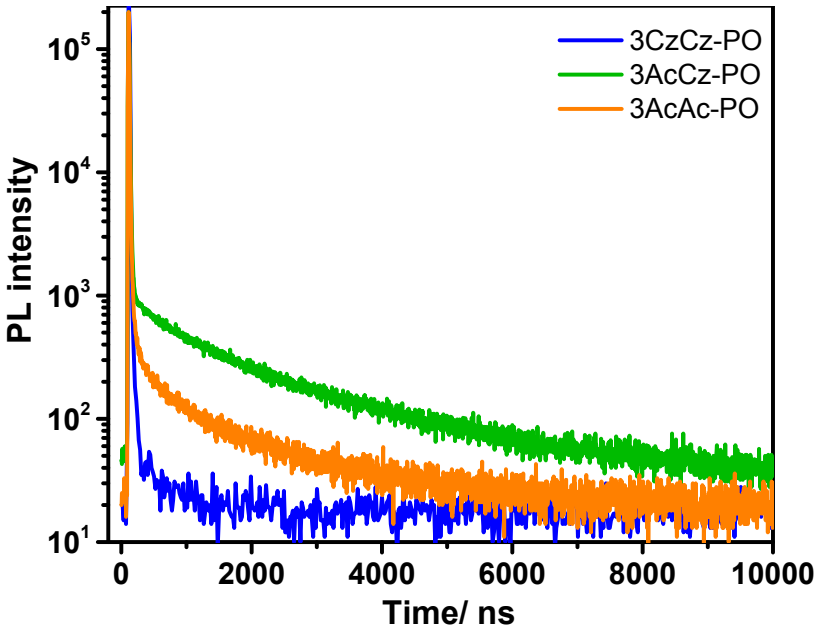

Figure 3. PL decay curves of 3CzCz-PO, 3AcCz-PO and 3AcAc-PO in film under nitrogen at 298 K.

View Article Online
DOI: 10.1039/C9TC03013A

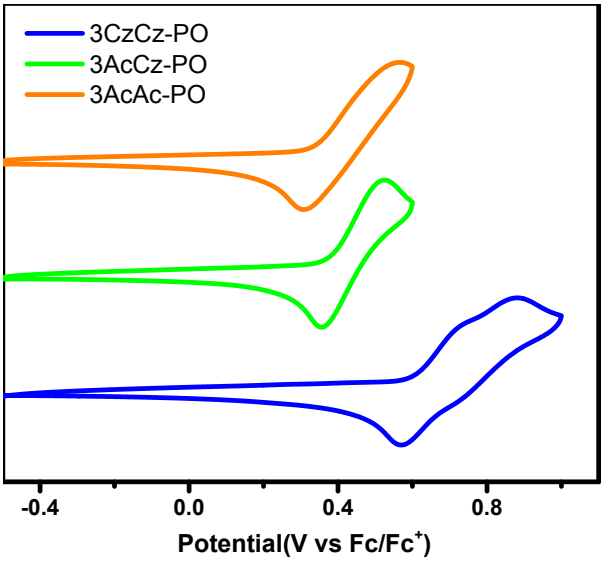

Figure 4. CV plots for 3CzCz-PO, 3AcCz-PO and 3AcAc-PO.

View Article Online
DOI: 10.1039/C9TC03013A

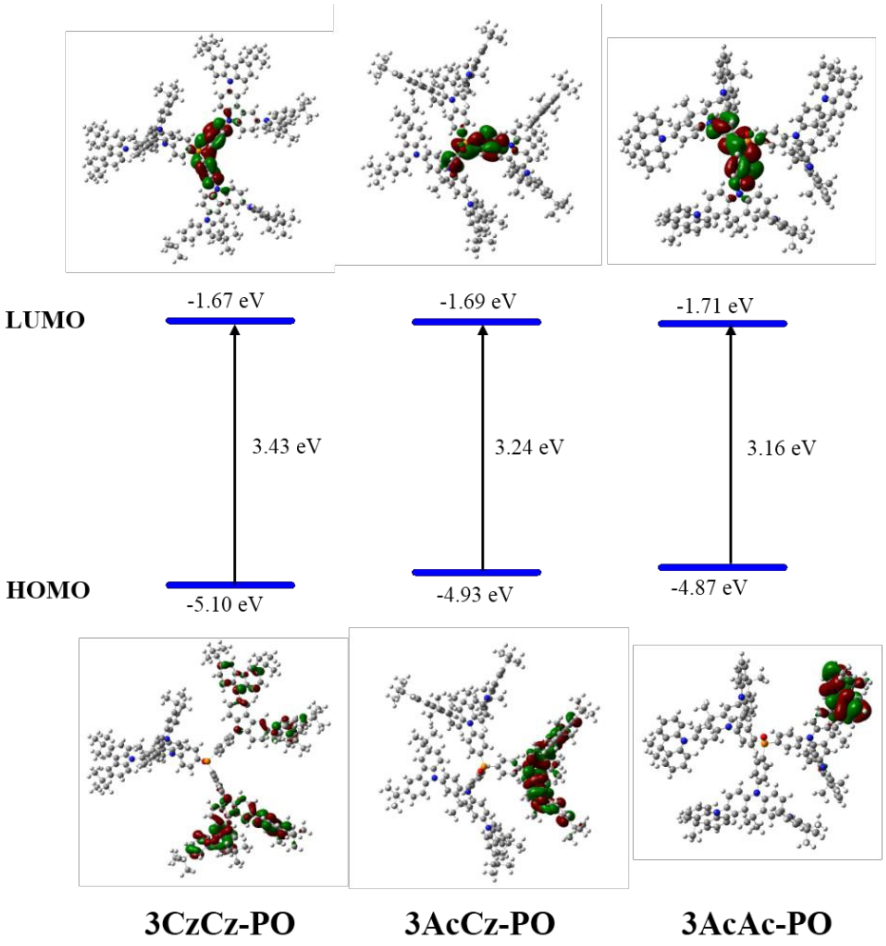

Figure 5. Frontier orbital distributions and energy levels of 3CzCz-PO, 3AcCz-PO and 3AcAc-PO calculated at the B3LYP/6-31G* level by Gaussian 09.

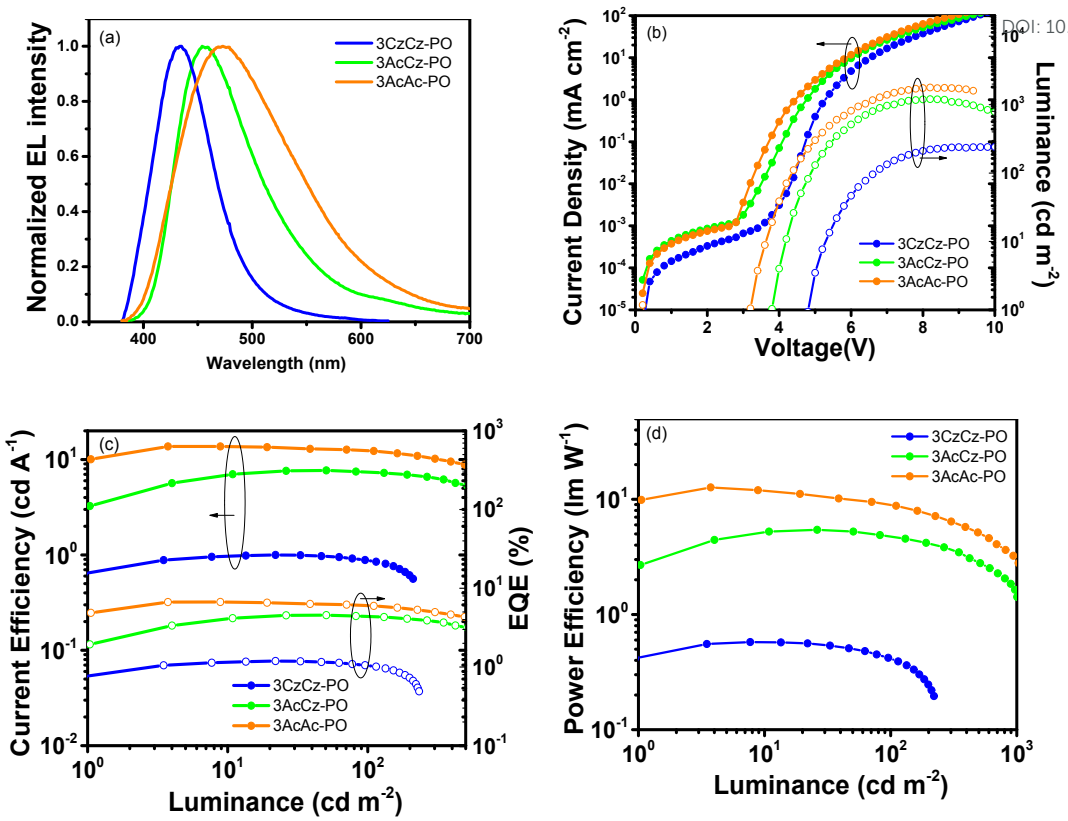

Figure 6. Non-doped device performance for 3CzCz-PO, 3AcCz-PO and 3AcAc-PO: (a) EL spectra at a driving voltage of 8 V; (b) current density-voltage-luminance curves; (c) current efficiency and EQE as a function of luminance; (d) power efficiency as a function of luminance.

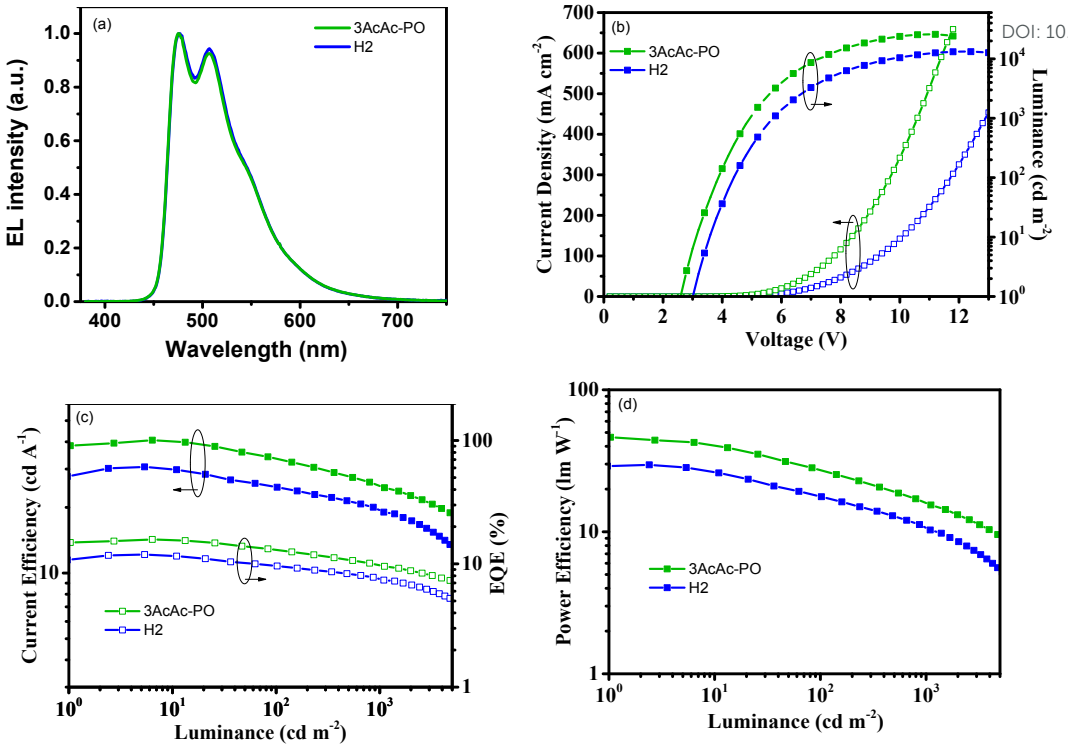

Figure 7. Device performance of 3AcAc-PO and H2 as host for 20wt% Ir(mpim)$_3$: (a) EL spectra at a driving voltage of 4 V; (b) current density-voltage-luminance curves; (c) current efficiency and EQE as a function of luminance; (d) power efficiency as a function of luminance.

View Article Online
DOI: 10.1039/C9TC03013A

Table 1. Photophysical, electrochemical and thermal properties for 3CzCz-PO, 3AcCz-PO and 3AcAc-PO.

	λ_{abs}(logε) [a] [nm]	λ_{em} [b] [nm]	Φ_{PL} [c] [%]	τ_p [d] [ns]	τ_d [d] [μs]	E_g [e] [eV]	HOMO [f] [eV]	LUMO [f] [eV]	S_1 [g] [eV]	T_1 [g] [eV]	ΔE_{st} [g] [eV]	T_d [h]/T_g [i] [°C]
3CzCz-PO	333 (4.84), 299 (5.17), 265 (5.21)	420	31	23	-	3.15	-5.40	-2.25	3.25	2.90	0.35	468/276
3AcCz-PO	314 (4.97), 299 (5.18), 265 (5.05)	454	22	31	1.5	2.89	-5.18	-2.29	3.08	2.87	0.22	431/157
3AcAc-PO	296 (5.17)	467	33	31	1.0	2.92	-5.13	-2.21	3.12	2.92	0.20	428/-

[a]Measured in 10^{-5} M CH_2Cl_2 solution. [b]Measured in film. [c]Measured in film with integrating sphere under N_2. [d]Lifetimes of prompt emission (τ_p) and delayed emission (τ_d) measured in film at 298 K in N_2. [e]The optical band gap estimated from the absorption onset. [f]HOMO=-e(E_{ox}^{onset} + 4.8 V), LUMO= HOMO + E_g , where E_{ox}^{onset} is the onset value of the first oxidation wave. [g]S_1 and T_1 of the dendrimers were calculated from the onset of the fluorescence and the phosphorescence spectra in films, and $\Delta E_{ST} = S_1 - T_1$. [h]Decomposition temperatures corresponding to a 5% weight loss. [i]Glass transition temperatures determined by DSC in N_2.

View Article Online
DOI: 10.1039/C9TC03013A

Table 2. EL performance of non-doped device and blue PhOLEDs.

EML	V_{on} [a] [V]	L_{max} [cd m^{-2}]	CE [b] [cd A^{-1}]	PE [b] [lm W^{-1}]	EQE [b] [%]	CIE [c] [x, y]
100% wt 3CzCz-PO	4.8	241	1.0	0.6	1.4	(0.18, 0.10)
100% wt 3AcCz-PO	3.8	1197	7.7	5.4	4.6	(0.20, 0.21)
100% wt 3AcAc-PO	3.2	1782	13.7	12.7	6.7	(0.21, 0.27)
3AcAc-PO: 20 wt.% $Ir(mpim)_3$	2.6	25815	40.7	46.4	15.8	(0.21, 0.44)
H2: 20 wt.% $Ir(mpim)_3$	3.0	13261	30.7	29.6	11.9	(0.21, 0.44)

[a]Turn-on voltage at a brightness of 1 cd m^{-2}; [b]Maximum values for current efficiency (CE), power efficiency (PE) and EQE, respectively; [c]CIE at 1000 cd m^{-2}.

View Article Online
DOI: 10.1039/C9TC03013A

Table of Contents Graphic